

# Synthesis and Structure of Two New High Nuclearity Ru/Pt Mixed-Metal Clusters

Brian F. G. Johnson,<sup>\*,[a]</sup> Sophie Hermans,<sup>[a]</sup> and Tetyana Khimyak<sup>[a]</sup>

**Keywords:** Cluster compounds / Ruthenium / Platinum / Heterometallic complexes / Bridging ligands

The reaction of the dianion  $[\text{Ru}_5\text{C}(\text{CO})_{14}]^{2-}$  with  $[\text{PtCl}_2(\text{MeCN})_2]$  in the presence of silica yields  $[\text{Ru}_5\text{PtC}(\text{CO})_{16}]$  (**1**) and the new compound  $[\text{PPN}]_2[\text{Ru}_{10}\text{Pt}_2\text{C}_2(\text{CO})_{28}]$  (**2**), while, in a related reaction,  $[\text{Ru}_6\text{C}(\text{CO})_{16}]^{2-}$  undergoes addition of  $[\text{PtCl}_2(\text{MeCN})_2]$  to yield the cluster  $[\text{Ru}_{12}\text{PtC}_2(\text{CO})_{32}]$

(**3**). The high nuclearity compounds **2** and **3** have been fully characterized and their structures determined by single crystal X-ray analysis.

(© Wiley-VCH Verlag GmbH & Co. KGaA, 69451 Weinheim, Germany, 2003)

## Introduction

Our recent success in the preparation of ruthenium-palladium mixed-metal nanoparticles which have been shown to possess high catalytic activity for a number of processes,<sup>[1]</sup> has led us to consider the possibility of extending our studies to embrace similar systems containing ruthenium and platinum. To this end, we have investigated the possibility of preparing appropriate high nuclearity derivatives based on both the  $\text{Ru}_5\text{C}$  and  $\text{Ru}_6\text{C}$  sub-cores, and which fall in the nanometer scale. In this paper we wish to report the synthesis and complete characterization of two such new high nuclearity clusters based on  $[\text{Ru}_{10}\text{Pt}_2\text{C}_2]$  and  $[\text{Ru}_{12}\text{PtC}_2]$  central units, one of which having already been used successfully as a nano-catalyst precursor.<sup>[2]</sup> These two compounds are reminiscent of the “sandwich” Ru-Pd clusters reported previously, which were obtained by reacting  $[\text{Ru}_6\text{C}(\text{CO})_{16}]^{2-}$  with  $[\text{Pd}(\text{MeCN})_4]^{2+}$ .<sup>[3]</sup> Our investigations have also led us to a potentially highly valuable method involving the use of silica as a “synthetic” reagent for the stabilization of highly active cationic metal fragments, a process that has already been reported elsewhere,<sup>[4]</sup> but is extended further here.

## Results and Discussion

When the salt  $[\text{PPN}]_2[\text{Ru}_5\text{C}(\text{CO})_{14}]$   $\{[\text{PPN}]^+ = \text{bis}(\text{triphenylphosphane})\text{iminium cation}\}$  was reacted with  $[\text{PtCl}_2(\text{MeCN})_2]$  in dichloromethane in the presence of silica, the solution darkened immediately. After separation by thin layer chromatography, two compounds were obtained. The first red compound was identified as the known  $[\text{Ru}_5\text{PtC}(\text{CO})_{16}]$  (**1**) on the basis of its mass and IR spec-

tra.<sup>[5]</sup> The second, brown, compound, isolated in 21% yield, was identified as  $[\text{PPN}]_2[\text{Ru}_{10}\text{Pt}_2\text{C}_2(\text{CO})_{28}]$  (**2**) on the basis of its mass spectrum, which shows a high intensity peak at  $m/z = 1104.7$  corresponding to half the mass of the anionic  $[\text{Ru}_{10}\text{Pt}_2\text{C}_2(\text{CO})_{28}]^{2-}$ . A weaker peak at  $m/z = 2209.4$  could be attributed to the same formulation, but only singly charged. The IR spectrum of **2** contains one broad peak at  $2026\text{ cm}^{-1}$  corresponding to terminal CO ligands and two weak peaks at  $1823$  and  $1789\text{ cm}^{-1}$  attributable to bridging carbonyls. Compound **2** could also be isolated as its  $\text{Ph}_4\text{P}^+$  salt, whose crystal structure is reported here. Crystals suitable for X-ray structure determination were obtained by slow diffusion of diethyl ether into a solution of **2** in dichloromethane. Compound **2** crystallises in the monoclinic space group  $P2_1/n$  and the molecular structure of the dianion  $[\text{Ru}_{10}\text{Pt}_2\text{C}_2(\text{CO})_{28}]^{2-}$  is presented in Figure 1, together with selected bond lengths and angles in Table 1.

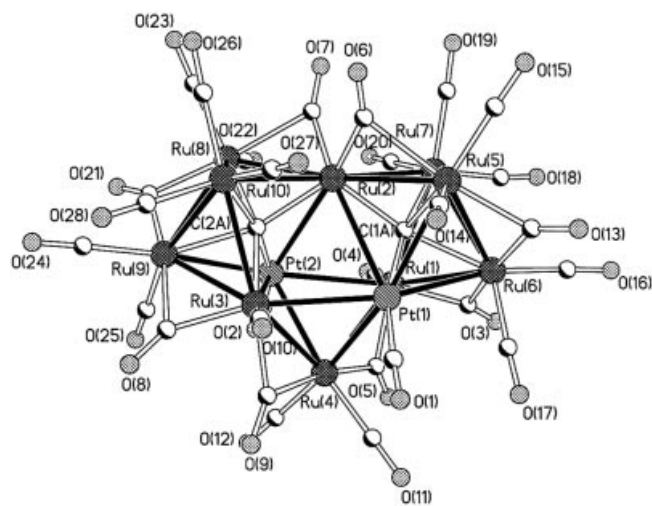


Figure 1. Molecular structure of the dianion  $[\text{Ru}_{10}\text{Pt}_2\text{C}_2(\text{CO})_{28}]^{2-}$  of **2** (labels on C atoms of carbonyl ligands correspond to those on O atoms and are omitted for clarity)

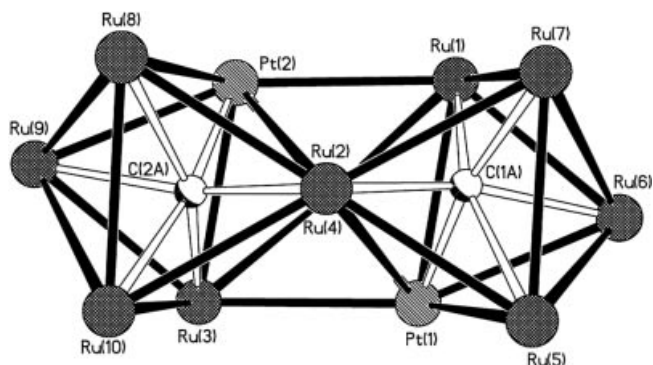
<sup>[a]</sup> University Chemical Laboratory,  
Lensfield Road, Cambridge CB2 1EW, UK

Table 1. Selected bond lengths (Å) and angles (°) for  $[\text{Ph}_4\text{P}]_2[\text{Ru}_{10}\text{Pt}_2\text{C}_2(\text{CO})_{28}]^{2-}$  (**2**)

Ru(2)–Pt(1)	3.0800(9)	Ru(5)–Ru(6)	2.8057(13)
Ru(4)–Pt(1)	2.7872(8)	Ru(6)–Ru(7)	2.9333(12)
Ru(2)–Pt(2)	3.1029(9)	Ru(8)–Ru(9)	2.7984(12)
Ru(4)–Pt(2)	2.7905(9)	Ru(9)–Ru(10)	2.9164(11)
Ru(2)–Ru(5)	2.8127(12)	Ru(2)–C(1a)	2.069(10)
Ru(2)–Ru(7)	2.8652(13)	Ru(2)–C(2a)	2.055(10)
Ru(2)–Ru(8)	2.7988(12)	Ru(6)–C(1a)	2.210(10)
Ru(2)–Ru(10)	2.8854(13)	Ru(9)–C(2a)	2.218(10)
Pt(1)–C(1a)–Ru(2)	96.7(5)	Pt(2)–C(2a)–Ru(2)	100.2(4)
Ru(1)–C(1a)–Ru(2)	114.7(4)	Ru(3)–C(2a)–Ru(2)	115.8(5)
Ru(1)–C(1a)–Ru(5)	161.9(6)	Ru(3)–C(2a)–Ru(8)	160.6(5)
Ru(2)–C(1a)–Ru(6)	162.9(5)	Ru(2)–C(2a)–Ru(9)	162.0(5)
Pt(1)–C(1a)–Ru(7)	169.6(5)	Pt(2)–C(2a)–Ru(10)	169.4(6)

The structure of the dianion of **2** may be viewed in two different ways. The first considers the cluster core as three square-based pyramidal units  $[\text{Pt}(1)\text{Ru}(1)\text{Ru}(5)\text{Ru}(6)\text{Ru}(7)]$ ,  $[\text{Pt}(1)\text{Pt}(2)\text{Ru}(1)\text{Ru}(3)\text{Ru}(4)]$ , and  $[\text{Pt}(2)\text{Ru}(3)\text{Ru}(8)\text{Ru}(9)\text{Ru}(10)]$  sharing two edges  $[\text{Pt}(1)\text{–Ru}(1)]$  and  $[\text{Pt}(2)\text{–Ru}(3)]$  and bound together through the Ru(2) atom. The two outer pyramids correspond to  $\text{Ru}_4\text{Pt}$  units whereas the central pyramid accounts for  $\text{Ru}_3\text{Pt}_2$ . Alternatively, the structure may be viewed as three face-sharing octahedra with the two common edges — Ru(1)–Ru(2) and Ru(3)–Ru(2) — missing. The Ru(1)–Ru(2) (3.475 Å) and Ru(2)–Ru(3) (3.511 Å) distances indicate little or no direct metal-metal bonding. All Pt–Ru distances are within the expected range<sup>[5,6]</sup> with the shortest being Pt(1)–Ru(4) and Pt(2)–Ru(4) [2.7872(8) and 2.7905(9) Å, respectively] and the longest Pt(1)–Ru(2) and Pt(2)–Ru(2) [3.0800(9) and 3.1029(9) Å, respectively]. The Ru–Ru distances are similar to those reported previously for hexanuclear ruthenium clusters,<sup>[7–9]</sup> and lie between 2.7984(12) Å and 2.9333(12) Å, with the shortest being Ru(8)–Ru(9) [2.7984(12) Å] and Ru(5)–Ru(6) [2.8057(13) Å] and the longest Ru(9)–Ru(10) [2.9164(11) Å] and Ru(6)–Ru(7) [2.9333(12) Å], all these belonging to the outer pyramids. The bases of the two outer pyramids are inclined at an angle of 40° with respect to each other. The interstitial carbon atoms in each of these pyramids are shifted towards the Ru(2) atom and deviate from the plane of the base [by –0.244 Å and 0.269 Å for C(1a) and C(2a), respectively]. In agreement with the infrared data, eight carbonyl ligands are in bridging mode while the remaining twenty are terminally bonded. The Ru(2) atom bears only two bridging carbonyl ligands — the Ru(7) and Ru(10) atoms have each three terminal carbonyls — but all the other Ru atoms bear two terminal CO ligands and share two bridging CO ligands with neighboring Ru atoms. The platinum atoms are connected only to terminal carbonyls. The overall symmetry of the anion is  $C_2$  with a twofold axis passing through Ru(2) and Ru(4) (Figure 2).

The cluster  $[\text{Ru}_{10}\text{Pt}_2\text{C}_2(\text{CO})_{28}]^{2-}$  (**2**) has a total of 166 valence electrons, which is four more than the 162 electrons predicted for three face-sharing octahedra, according to the

Figure 2. View down the  $C_2$  axis passing through Ru(2) (top) and Ru(4) (bottom) atoms of the metal core of the dianion **2**

condensed polyhedra approach proposed by Mingos. The four additional electrons might account for the two non-existing Ru–Ru bonds. This has also been noted in other Ru–Pt mixed-metal clusters, such as  $[\text{PtRu}_5\text{C}(\text{CO})_{13}(\mu\text{-RC}_2\text{R})(\mu_3\text{-RC}_2\text{R})]$  ( $\text{R} = \text{Et}$ ,<sup>[6]</sup>  $\text{Ph}^{[10]}$ ) with a capped square-based-pyramidal metal core. These compounds have a total electron count of 88, which is two more than predicted by the PSEPT rules and is accounted for by the presence of two unusually long, and consequently weakened, Ru–Ru bonds.

The formation mechanism of compound **2** is unclear. The silica present in the reaction mixture is presumed to assist the formation of the active fragment  $[\text{Pt}(\text{MeCN})_2]^{2+}$ , which undergoes addition to  $[\text{Ru}_5\text{C}(\text{CO})_{14}]^{2-}$  (by analogy with the reactions involving  $[\text{PtCl}_2(\text{COD})]$ , see ref.<sup>[4])</sup>. The hypothetical monomer  $[\text{Ru}_5\text{PtC}(\text{CO})_{14}(\text{MeCN})_2]$  is probably unstable and readily undergoes rearrangement to form compounds **1** and **2**. The fact that the ratio of the two metals in **2** is 10:2 is consistent with this view involving as it does prior formation of a  $\text{Ru}_5\text{Pt}$  adduct. The same product,  $[\text{Ru}_{10}\text{Pt}_2\text{C}_2(\text{CO})_{28}]^{2-}$ , was obtained when  $[\text{PPN}]_2[\text{Ru}_5\text{C}(\text{CO})_{14}]$  was reacted with  $[\text{PtCl}_2(\text{PhCN})_2]$  in dichloromethane in the presence of silica. Its identity was proven by infrared spectroscopy and mass spectrometry. This result further supports our view on the mechanism of formation of **2**.

If the reaction leading to the formation of **2** does follow the proposed mechanism, then the formation of  $[\text{Ru}_5\text{PtC}(\text{CO})_{16}]$  (**1**) would be dependent upon the availability of CO that could substitute the acetonitrile in the intermediate (the simple adduct formed initially). Therefore, a reaction of  $[\text{Ru}_5\text{C}(\text{CO})_{14}]^{2-}$  with  $[\text{PtCl}_2(\text{MeCN})_2]$  was carried out under an atmosphere of carbon monoxide. Indeed, compound **1** was isolated in 11% yield, to compare with 1.7% obtained from the reaction carried out under  $\text{N}_2$ . The second product isolated was identified as  $[\text{PPN}]_2[\text{Ru}_{10}\text{Pt}_3\text{C}_2(\text{CO})_{32}]$ . The detailed synthesis and structure of this compound will be reported elsewhere.<sup>[11]</sup>

Similarly, in an alternative set of experiments, we find that when the salt  $[\text{PPN}]_2[\text{Ru}_6\text{C}(\text{CO})_{16}]$  is treated with the same platinum compound,  $[\text{PtCl}_2(\text{MeCN})_2]$ , in dichloromethane, in the presence of silica, a high nuclearity cluster is

also obtained. In this case the product was found to be  $[\{\text{Ru}_6\text{C}(\text{CO})_{16}\}_2\text{Pt}(\text{MeCN})_2]$  (**3**) on the basis of a single crystal X-ray structure determination. In its infrared spectrum, bands attributable to both terminal (2076 and 2002  $\text{cm}^{-1}$ ) and bridging CO ligands (1869 and 1844  $\text{cm}^{-1}$ ) were observed. In the  $^1\text{H}$  NMR spectrum, recorded in  $\text{CD}_2\text{Cl}_2$ , two peaks, at  $\delta = 1.32$  (3 H) and 0.89 (3 H) ppm, may be assigned to the two MeCN ligands. In the mass spectrum, a molecular peak was not observed, but instead a peak at  $m/z = 1096$  corresponding to  $[\text{Ru}_6\text{C}(\text{CO})_{17}]$  was found. Crystals suitable for X-ray diffraction structure determination were grown by slow diffusion of hexane into a solution of **3** in dichloromethane. The structure obtained is shown in Figure 3 and relevant bond lengths and angles are listed in Table 2.

The asymmetric unit of the crystal structure contains two independent but structurally similar molecules. The overall molecular structure of **3** consists of two  $[\text{Ru}_6\text{C}(\text{CO})_{16}]$  octahedra linked by a single Pt atom and one bridging acetonitrile ligand (Figure 4). This MeCN ligand forms an unusual triple bridge, linked through its nitrogen atom to the platinum and one ruthenium atom  $[\text{Ru}(10)]$ , and through

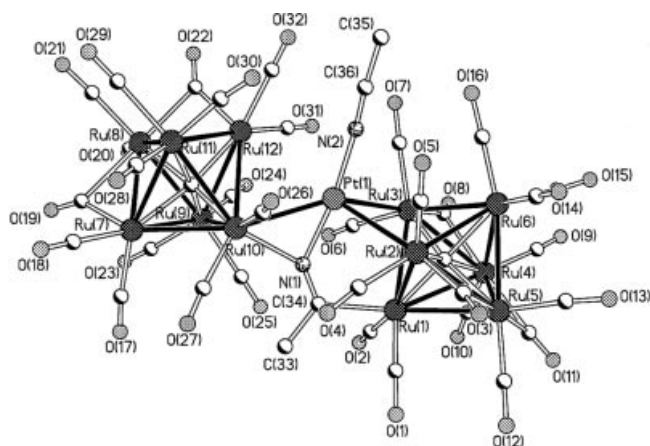


Figure 3. Molecular structure of  $[\{\text{Ru}_6\text{C}(\text{CO})_{16}\}_2\text{Pt}(\text{MeCN})_2]$  (**3**) (labels on C atoms of carbonyl ligands correspond to those on O atoms and are omitted for clarity)

the carbon to a second ruthenium atom  $[\text{Ru}(1)]$ . A second acetonitrile ligand is terminally bound to the platinum atom through its nitrogen lone pair. The  $\text{Ru}(2) - \text{Ru}(3)$  distance in one of the  $\text{Ru}_6$  octahedra is beyond the range usually considered as a Ru–Ru bond. A compound in which two  $\text{Ru}_3$  cluster subunits are linked by a single platinum atom has been previously reported but is of lower nuclearity ( $\text{Ru}_3\text{-Pt-Ru}_3$ ).<sup>[12]</sup> The geometry of the two  $[\text{Ru}_6\text{C}(\text{CO})_{16}]$  moieties in **3** is not unusual, except for the “missing” Ru–Ru edge. The two carbide atoms lie at the centre of the octahedra. The Ru–Ru bond lengths range from 2.806(2) to 3.114(2) Å in molecule 1 and from 2.803(2) to 3.085(2) Å in molecule 2. These span a wider range than those found in  $[\text{Ru}_6\text{C}(\text{CO})_{17}]$  [2.827(5)–3.034(5) Å], but average to the same value (ca. 2.90 Å).<sup>[5]</sup> Three carbonyl ligands bridge Ru–Ru edges in the first  $\text{Ru}_6$  unit [containing the long  $\text{Ru}(2) - \text{Ru}(3)$  bond], while only two occupy a bridging position in the second  $\text{Ru}_6$  unit. All the other carbonyl ligands are terminal and almost linear. The Ru–Ru edges spanned by bridging CO ligands are amongst the shortest. The longest Ru–Ru edges are associated with the Ru atoms bonded to the bridging acetonitrile ligand  $[\text{Ru}(1)$  and  $\text{Ru}(10)]$ , which is presumably due to the increased electron density on these atoms. The Ru–Pt distances vary from 2.7412(14) to 2.8734(12) Å in molecule 1 and from 2.7562(12) to 2.8897(13) Å in molecule 2. As such there are two short and one longer Ru–Pt bonds. These distances are very similar to the mean value (2.789 Å) that can be calculated over all the compounds containing a Ru–Pt bond that have been characterised crystallographically. The MeC–N bond length in the acetonitrile ligand bound in a terminal fashion is 1.16(2) Å in molecule 1 and 1.17(2) Å in molecule 2. These values are typical of a  $\text{C}\equiv\text{N}$  triple bond (theoretical value: 1.16 Å) and fall within the range [1.03(7)–1.22(8) Å] reported for a number of “end-on” nitrile complexes characterised by X-ray crystallography.<sup>[13]</sup> The second acetonitrile ligand is not linear: the  $\text{Pt} - \text{N} - \text{C}$  angle is  $133.9(10)^\circ$  in molecule 1 and  $131.6(10)^\circ$  in molecule 2, while the  $\text{N} - \text{C} - \text{CH}_3$  angle is  $120.1(13)^\circ$  in molecule 1 and  $120.5(12)^\circ$  in molecule 2. The MeC–N distance of 1.28(2) Å in both molecules is

Table 2. Selected bond lengths (Å) and angles ( $^\circ$ ) for  $[\{\text{Ru}_6\text{C}(\text{CO})_{16}\}_2\text{Pt}(\text{MeCN})_2]$  (**3**)

	Molecule 1	Molecule 2		Molecule 1	Molecule 2
$\text{Ru}(3) - \text{Pt}(1)$	2.7769(13)	2.7882(12)	$\text{Ru}(2) - \text{Pt}(1) - \text{N}(2)$	94.1(3)	97.3(3)
$\text{Ru}(2) - \text{Pt}(1)$	2.8734(12)	2.8897(13)	$\text{Ru}(3) - \text{Pt}(1) - \text{N}(2)$	97.6(3)	93.4(3)
$\text{Ru}(10) - \text{Pt}(1)$	2.7412(14)	2.7562(12)	$\text{Ru}(2) - \text{Pt}(1) - \text{Ru}(3)$	71.36(3)	71.17(4)
$\text{Pt}(1) - \text{N}(1)$	1.963(12)	1.949(11)	$\text{Ru}(2) - \text{Pt}(1) - \text{N}(1)$	87.4(3)	87.2(3)
$\text{Pt}(1) - \text{N}(2)$	1.990(13)	1.990(13)	$\text{Ru}(3) - \text{Pt}(1) - \text{N}(1)$	95.1(3)	97.2(3)
$\text{N}(2) - \text{C}(36)$	1.16(2)	1.17(2)	$\text{Ru}(10) - \text{Pt}(1) - \text{N}(1)$	50.5(3)	49.0(3)
$\text{C}(36) - \text{C}(35)$	1.53(2)	1.43(2)	$\text{Ru}(10) - \text{Pt}(1) - \text{N}(2)$	119.1(3)	120.7(3)
$\text{N}(1) - \text{C}(34)$	1.28(2)	1.28(2)	$\text{Ru}(10) - \text{Pt}(1) - \text{Ru}(2)$	122.14(4)	117.74(4)
$\text{N}(1) - \text{Ru}(10)$	2.127(10)	2.086(11)	$\text{Ru}(10) - \text{Pt}(1) - \text{Ru}(3)$	137.53(4)	141.05(4)
$\text{C}(34) - \text{C}(33)$	1.49(2)	1.53(2)	$\text{N}(1) - \text{Pt}(1) - \text{N}(2)$	167.0(5)	169.3(4)
$\text{C}(34) - \text{Ru}(1)$	2.081(13)	2.116(14)	$\text{Pt}(1) - \text{N}(2) - \text{C}(36)$	175.4(13)	177.8(12)
$\text{C} - \text{O}$ (mean)	1.154(4)	1.146(3)	$\text{N}(2) - \text{C}(36) - \text{C}(35)$	176.8(17)	176.8(16)
			$\text{Pt}(1) - \text{N}(1) - \text{C}(34)$	133.9(10)	131.6(10)
			$\text{N}(1) - \text{C}(34) - \text{C}(33)$	120.1(13)	120.5(12)

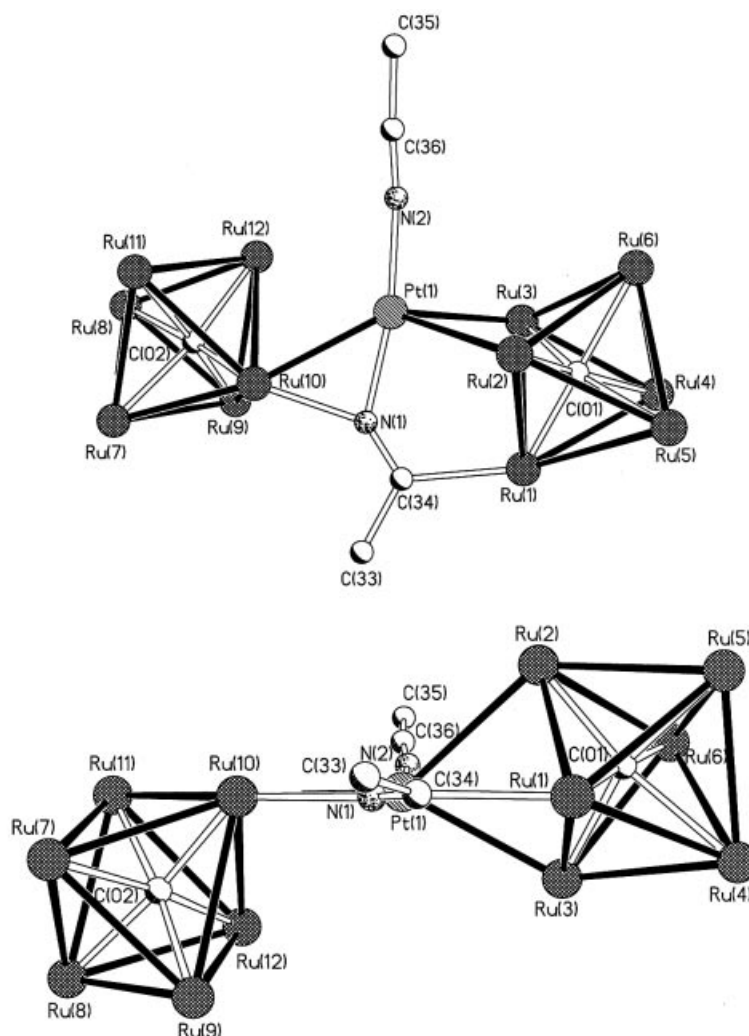


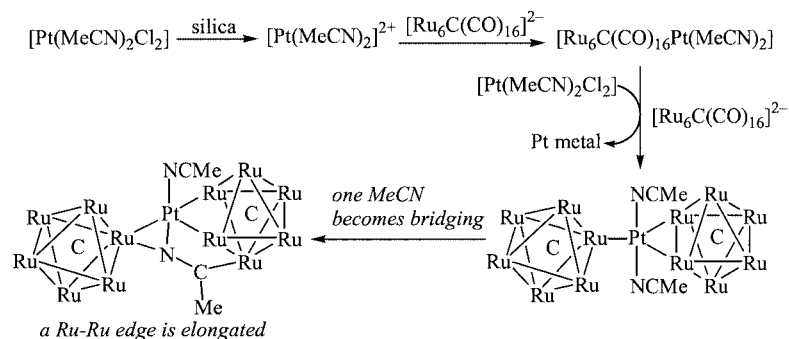
Figure 4. Side views of the structure of  $[\{\text{Ru}_6\text{C}(\text{CO})_{16}\}_2\text{Pt}(\text{MeCN})_2]$  (**3**), emphasising the coordination of both MeCN ligands (top) and the planarity of the bridging acetonitrile ligand (bottom); carbonyl ligands are omitted for clarity

typical of a C=N double bond (theoretical value: 1.28 Å). These angles (close to the ideal  $120^\circ$  value) and bond length indicate that the C(34) and N(1) atoms are  $sp^2$  rehybridised in the bridging MeCN. Indeed, the N-C atoms of the ligand are coplanar with the bridged platinum and two ruthenium atoms. The view shown in Figure 4 (bottom) emphasises the planarity of the bridging acetonitrile.

This type of triply bridging nitrile ligand has been reported only in one previous instance, in the compound  $[\text{Os}_6\text{Pt}(\text{CO})_{17}(\text{NCMe})(\text{COD})]$ .<sup>[14]</sup> The C–N bond length in that case was intermediate between a triple and a double bond [1.22(3) Å], and the distribution of metal-metal bonds between the atoms bridged by the MeCN unit was different. The bridging nitrile was considered to be a four-electron donor. The shift of the second MeCN ligand in  $[\{\text{Ru}_6\text{C}(\text{CO})_{16}\}_2\text{Pt}(\text{MeCN})_2]$  (**3**) from a terminal to a triply bridging bonding mode is thus accompanied by a change from a two-electron donor to a four-electron donor capacity. This additional pair of available electrons might explain the observed lengthening of one Ru–Ru distance in one of the octahedra. The  $\text{Ru}_6$  unit displaying this elong-

ated Ru–Ru distance is associated with the greatest number of interactions with the platinum fragment (two Ru–Pt bonds and one Ru–N bond, as opposed to one Ru–Pt and one Ru–N bond for the other  $\text{Ru}_6$  unit). The coordination geometry at the platinum atom can be described either as a distorted trigonal bipyramid [N(1) and N(2) axials] or a distorted square pyramid [Ru(2) axial]. A five-coordinate Pt atom is indicative of the metal centre being in the +2 oxidation state,<sup>[15]</sup> and non-planar  $\text{Pt}^{\text{II}}$  usually respects the 18-electron rule. Indeed, in **3**, eight electrons are provided by the platinum, and each of the three Pt–Ru bonds accounts for two electrons, as do each of the two Pt–N bonds, reaching a total of 18 around the Pt atom. The oxidation state of the platinum is thus unchanged during the course of the reaction. If the reaction is considered as the addition of two  $[\text{Ru}_6\text{C}(\text{CO})_{16}]^{2-}$  “ligands” to the  $[\text{Pt}(\text{MeCN})_2]^{2+}$  fragment, the resulting adduct should be doubly negatively charged. An oxidation of one  $[\text{Ru}_6\text{C}(\text{CO})_{16}]^{2-}$  unit to  $[\text{Ru}_6\text{C}(\text{CO})_{16}]$  must have occurred, probably at the expense of some  $[\text{PtCl}_2(\text{MeCN})_2]$  undergoing reduction to platinum(0). This would explain the low





Scheme 1. Suggested mechanism for the reaction leading to  $[\{\text{Ru}_6\text{C}(\text{CO})_{16}\}_2\text{Pt}(\text{MeCN})_2]$  (**3**); carbonyl ligands are omitted for clarity

yield of the reaction. Scheme 1 summarises our view on the mechanism of the reaction leading to the formation of  $[\{\text{Ru}_6\text{C}(\text{CO})_{16}\}_2\text{Pt}(\text{MeCN})_2]$  (**3**).

## Conclusions

In this paper we have reported the synthesis of two high nuclearity Ru-Pt clusters, obtained by reacting  $[\text{Ru}_5\text{C}(\text{CO})_{14}]^{2-}$  or  $[\text{Ru}_6\text{C}(\text{CO})_{16}]^{2-}$  with  $[\text{PtCl}_2(\text{MeCN})_2]$  in the presence of silica. The idea that  $[\text{Ru}_5\text{C}(\text{CO})_{14}]^{2-}$  and  $[\text{Ru}_6\text{C}(\text{CO})_{16}]^{2-}$  may serve as simple bidentate ligands (for the platinum) in a conventional sense is attractive and has certainly been of benefit previously in our interpretation of the chemistry of certain Ru-Sn systems.<sup>[16]</sup> Here this view is complicated by further reaction, leading to rearrangement of the cluster core in **2** and the formation of a triply bridging MeCN ligand in **3**. Additionally, in these reactions, the role of the silica is crucial and its net action is to remove  $\text{Cl}^-$ . High yields of other Ru-Pt clusters of predictable nuclearity were obtained following this method,<sup>[4]</sup> while the use of more conventional chloride scavengers (such as  $\text{AgBF}_4$ ) did not prove as efficient. No reaction is observed in the absence of silica, leading to the conclusion that an initial reaction of  $[\text{PtCl}_2(\text{MeCN})_2]$  with surface Si-OH occurs, resulting in surface-bonded and stabilised  $[\text{Pt}(\text{MeCN})_2]^{2+}$  units, that can then react with the ruthenium clusters in a controlled way. This aspect is under further exploration.

## Experimental Section

All the reactions were carried out using standard Schlenk techniques, under water- and oxygen-free nitrogen. All solvents were dried and distilled immediately before use. Reactants and chemicals were purchased from Aldrich Chemicals and used without further purification. The silica used in reaction media was Silica gel 60 (0.040–0.063 mm) for column chromatography purchased from Merck. The clusters  $[\text{PPN}]_2[\text{Ru}_5\text{C}(\text{CO})_{14}]^{17}$  and  $[\text{PPN}]_2[\text{Ru}_6\text{C}(\text{CO})_{16}]^{18}$  were synthesised following literature procedures.

All chromatographic separations were performed on the open bench without any precaution to exclude air. Thin-layer chromatography (TLC) was carried out using glass plates (20 × 20 cm) co-

ated with a layer of silica gel 60 F<sub>254</sub>, supplied by Merck. The eluents used were standard grade laboratory solvents.

Infrared spectra were collected in dichloromethane solution using a NaCl liquid cell (0.5 mm path length) supplied by Specac Ltd., on a Perkin–Elmer Paragon 1000 FT-IR spectrometer. The mass spectra were obtained on a Kratos Concept spectrometer (\*) using electron impact ionisation (EI) in positive mode or on a Micromass Quattro-LC spectrometer using the electrospray ionisation technique (ESI) in negative mode (†). The <sup>1</sup>H NMR spectrum was recorded on a Bruker DPX-400 instrument. The elemental analyses were performed by the microanalysis service of the department.

**Preparation of  $[\text{Ru}_5\text{PtC}(\text{CO})_{16}]$  (**1**) and  $[\text{PPN}]_2[\text{Ru}_{10}\text{Pt}_2\text{C}_2(\text{CO})_{28}]$  (**2**):**  $[\text{PPN}]_2[\text{Ru}_5\text{C}(\text{CO})_{14}]$  (100 mg, 0.050 mmol) was dissolved in dichloromethane (20 mL). A slight excess of  $[\text{PtCl}_2(\text{MeCN})_2]$  (20 mg, 0.057 mmol) and two spoons of silica (ca. 1 g) were added, inducing an immediate darkening of the solution. After five hours stirring at room temperature, the mixture was filtered, and the solvent evaporated. The residue was separated into its component compounds by thin layer chromatography, using hexane/acetone/dichloromethane (50:5:45, v/v) as eluent. The top orange band was identified as  $[\text{Ru}_5\text{PtC}(\text{CO})_{16}]$  (**1**), obtained in very low yield (1 mg, 1.7%), and  $[\text{PPN}]_2[\text{Ru}_{10}\text{C}_2\text{Pt}_2(\text{CO})_{28}]$  (**2**) (17 mg, 21%) was isolated from the bottom. Compound **2** can also be isolated as its  $[\text{Ph}_4\text{P}]^+$  salt.

**$[\text{Ru}_5\text{PtC}(\text{CO})_{16}]$  (**1**):** IR ( $\text{CH}_2\text{Cl}_2$ ):  $\nu_{\text{CO}}$  2065.0(s), 2049.7(vs), 2003.0(w, sh), 1873.1(vw, br)  $\text{cm}^{-1}$ . EI-MS (\*):  $m/z$  = 1163 (calcd. for  $\text{Ru}_5\text{PtC}(\text{CO})_{16}$ : 1162,  $M^+$ ), followed by loss of 16 CO ligands.

**$[\text{Ph}_4\text{P}]_2[\text{Ru}_{10}\text{Pt}_2\text{C}_2(\text{CO})_{28}]$  (**2**):** IR ( $\text{CH}_2\text{Cl}_2$ ):  $\nu_{\text{CO}}$  2026vs (br), 2002m (sh), 1964w (sh), 1823m (br), 1789m (br)  $\text{cm}^{-1}$ . ESI-MS (†):  $m/z$  = 1104.7 (calcd. for  $[\text{Ru}_{10}\text{Pt}_2\text{C}_2(\text{CO})_{28}]^{2-}$ : 1104.6,  $M^{2-}/2$ ), 2209.4 (calcd. for  $[\text{Ru}_{10}\text{Pt}_2\text{C}_2(\text{CO})_{28}]^-$ : 2209.2,  $M^-$ ).  $\text{C}_{78}\text{H}_{40}\text{O}_{28}\text{P}_2\text{Pt}_2\text{Ru}_{10}$  (2888.0): calcd. C 32.44, H 1.40; found C 32.26, H 1.56.

**Reaction of  $[\text{PPN}]_2[\text{Ru}_5\text{C}(\text{CO})_{14}]$  with  $[\text{Pt}(\text{PhCN})_2\text{Cl}_2]$ :**  $[\text{PPN}]_2[\text{Ru}_5\text{C}(\text{CO})_{14}]$  (100 mg, 0.050 mmol) was dissolved in dichloromethane (20 mL). An equivalent of  $[\text{PtCl}_2(\text{PhCN})_2]$  (24 mg, 0.050 mmol) and two spoons of silica (ca. 1 g) were added, inducing an immediate darkening of the solution. After five hours stirring at room temperature, the mixture was filtered, and the solvent evaporated. The residue was separated into its component compounds by thin layer chromatography, using hexane/acetone/dichloromethane (40:20:40, v/v) as eluent. The top orange band was identified as  $[\text{Ru}_5\text{PtC}(\text{CO})_{16}]$  (**1**), obtained in very low yield (less than 1 mg), and  $[\text{PPN}]_2[\text{Ru}_{10}\text{C}_2\text{Pt}_2(\text{CO})_{28}]$  (**2**) (21 mg, 26%) was isolated from the bottom.

**Reaction of  $[\text{PPN}]_2[\text{Ru}_5\text{C}(\text{CO})_{14}]$  with  $[\text{PtCl}_2(\text{MeCN})_2]$  under CO:** One equivalent of  $[\text{PtCl}_2(\text{MeCN})_2]$  (18 mg, 0.05 mmol) and silica

Table 3. Crystal data for [Ph<sub>4</sub>P]<sub>2</sub>[Ru<sub>10</sub>Pt<sub>2</sub>C<sub>2</sub>(CO)<sub>28</sub>] (**2**) and [{Ru<sub>6</sub>C(CO)<sub>16</sub>}<sub>2</sub>Pt(MeCN)<sub>2</sub>] (**3**)

	<b>2</b>	<b>3</b>
Chemical formula	C <sub>78</sub> H <sub>40</sub> O <sub>28</sub> P <sub>2</sub> Pt <sub>2</sub> Ru <sub>10</sub>	C <sub>38.75</sub> H <sub>7.50</sub> Cl <sub>1.50</sub> N <sub>2</sub> O <sub>32</sub> PtRu <sub>12</sub>
Mol. wt.	2887.92	2474.07
Wavelength (Å)	0.71073	0.71069
<i>T</i> (K)	180(2)	180(2)
Crystal size (mm)	0.32 × 0.12 × 0.02	0.18 × 0.07 × 0.01
Crystal system	monoclinic	monoclinic
Space group	<i>P</i> 2 <sub>1</sub> / <i>n</i>	<i>P</i> 2 <sub>1</sub> / <i>c</i>
<i>a</i> (Å)	21.8793(5)	10.392(2)
<i>b</i> (Å)	14.2035(3)	44.191(3)
<i>c</i> (Å)	28.6527(7)	24.911(2)
β (°)	111.3430(10)	98.9(3)
<i>V</i> (Å <sup>3</sup> )	8293.5(3)	11299.4(3)
<i>Z</i>	4	8
<i>D</i> <sub>calc</sub> (mg m <sup>−3</sup> )	2.313	2.909
μ (mm <sup>−1</sup> )	5.204	5.737
<i>F</i> (000)	5432	9132
2θ range (deg)	7.12 – 54.96	2.48 – 50.02
No. of reflections collected	41483	30770
No. of indep reflections	18548	18539
<i>R</i> <sub>int</sub>	0.0798	0.0716
Refinement method	full-matrix least-square on <i>F</i> <sup>2</sup>	full-matrix least-square on <i>F</i> <sup>2</sup>
Refined parameters	1005	845
Goodness of fit on <i>F</i> <sup>2</sup>	1.027	0.997
Final <i>R</i> indices [ <i>I</i> > 2σ( <i>I</i> )]		
<i>R</i> 1, <sup>[a]</sup> <i>wR</i> 2 <sup>[b]</sup>	0.0607, 0.1249	0.0553, 0.1029
(all data)	0.1253, 0.1472	0.1255, 0.2073
Largest diff peak/hole (e <sup>−</sup> Å <sup>−3</sup> )	2.813/−1.338	2.214/−1.915

<sup>[a]</sup> *R*1 = Σ*F*<sub>o</sub> − *F*<sub>c</sub>/Σ*F*<sub>o</sub>. <sup>[b]</sup> *wR*2 = [Σ*w*(*F*<sub>o</sub><sup>2</sup> − *F*<sub>c</sub><sup>2</sup>)/Σ*w*(*F*<sub>o</sub><sup>2</sup>)<sup>1/2</sup>].

(approx. 1 g) were added to a solution of [PPN]<sub>2</sub>[Ru<sub>5</sub>C(CO)<sub>14</sub>] (100 mg, 0.05 mmol) in CH<sub>2</sub>Cl<sub>2</sub> (20 mL). The mixture was stirred for 3 hours under carbon monoxide and then left to stir overnight under nitrogen. Subsequently, the silica was filtered off and the solvent evaporated to dryness in vacuo. The crude product was dissolved in a minimum amount of CH<sub>2</sub>Cl<sub>2</sub> and purified by TLC using a mixture of CH<sub>2</sub>Cl<sub>2</sub>/acetone/hexane (45:5:50, v/v) as eluent. The top red band was identified as [PtRu<sub>5</sub>C(CO)<sub>16</sub>] (**1**) (11 mg, 0.009 mmol, 19% yield) and the bottom violet band was identified as [PPN]<sub>2</sub>[Pt<sub>3</sub>Ru<sub>10</sub>C<sub>2</sub>(CO)<sub>32</sub>] (4 mg, 0.001 mmol, 2.5% yield).

[Ru<sub>5</sub>PtC(CO)<sub>16</sub>] (**1**): IR (CH<sub>2</sub>Cl<sub>2</sub>): ν<sub>CO</sub> 2064.5(s), 2049.9(vs), 2004(w, sh), 1869(vw, br) cm<sup>−1</sup>. EI-MS (\*): *m/z* = 1162 (calcd. for Ru<sub>5</sub>PtC(CO)<sub>16</sub>: 1162, *M*<sup>+</sup>), followed by loss of 16 CO ligands.

**Preparation of [{Ru<sub>6</sub>C(CO)<sub>16</sub>]<sub>2</sub>Pt(MeCN)<sub>2</sub>] (**3**):** The reaction was performed in a similar fashion, starting from [PPN]<sub>2</sub>[Ru<sub>6</sub>C(CO)<sub>16</sub>] (100 mg, 0.0466 mmol) and [PtCl<sub>2</sub>(MeCN)<sub>2</sub>] (16 mg, 0.0466 mmol) and purification by thin-layer chromatography, using hexane/dichloromethane (3:2, v/v) as eluent. The eluting brown fraction is [{Ru<sub>6</sub>C(CO)<sub>16</sub>]<sub>2</sub>Pt(MeCN)<sub>2</sub>] (**3**), obtained in very low yield (3.4 mg, 3.03%).

[{Ru<sub>6</sub>C(CO)<sub>16</sub>]<sub>2</sub>Pt(MeCN)<sub>2</sub>] (**3**): IR (CH<sub>2</sub>Cl<sub>2</sub>): ν<sub>CO</sub> 2076(m), 2063(s), 2048(vs), 2018 (w, sh), 2002(w, sh), 1869(w, br), 1844(w, br) cm<sup>−1</sup>. <sup>1</sup>H NMR (400 MHz, CD<sub>2</sub>Cl<sub>2</sub>, 25 °C): δ = 0.89 (s, 3 H, MeCN), 1.32 (s, 3 H, MeCN) ppm. EI-MS (\*): *m/z* = 1096 (calcd. for Ru<sub>6</sub>C(CO)<sub>17</sub>: 1095), with CO losses. C<sub>38</sub>H<sub>6</sub>N<sub>2</sub>O<sub>32</sub>Pt<sub>1</sub>Ru<sub>12</sub> (2410.4): calcd. C 18.94, H 0.25, N 1.16; found C 21.40, H 3.17, N 0.33. Crystals suitable for X-ray diffraction structure determination were grown by slow diffusion of hexane into a solution of **3** in dichloromethane.

**Crystallography:** Single crystal X-ray diffraction analyses were performed on a Nonius Kappa CCD system with a sealed-tube Mo-*K*<sub>α</sub> source equipped with an Oxford Cryostream apparatus for low-temperature data collection. The structures were solved by direct methods using teXsan,<sup>[18]</sup> and refined by full-matrix least-squares on *F*<sup>2</sup> with the SHELXL-97<sup>[19]</sup> (**2**) and SHELXL-93<sup>[20]</sup> (**3**) software packages. In the case of **2**, all non-hydrogen atoms, apart from the solvent molecules and disordered groups (one of the Ph<sub>4</sub>P cations is disordered over two positions), were refined with anisotropic atomic displacement parameters. In the case of **3**, only the Ru and Pt metal atoms were refined with anisotropic atomic displacement parameters. All hydrogen atoms were placed in idealised positions, assigned isotropic displacement parameters and allowed to ride on the parent carbons. The crystal data for **2** and **3** are summarised in Table 3.

CCDC-191419 (**2**) and 191420 (**3**) contain the supplementary crystallographic data for this paper. These data can be obtained free of charge at [www.ccdc.cam.ac.uk/conts/retrieving.html](http://www.ccdc.cam.ac.uk/conts/retrieving.html) [or from the Cambridge Crystallographic Data Centre, 12 Union Road, Cambridge CB2 1EZ, UK; fax: (internat.) +44-1223/336-033; E-mail: [deposit@ccdc.cam.ac.uk](mailto:deposit@ccdc.cam.ac.uk)].

## Acknowledgments

We are very grateful to John E. Davies and Andrew D. Bond for data collection for compounds **2** and **3** and structure refinement for compound **3**, and to the European Commission and Newnham College, Cambridge, for funding to SH, to the Cambridge Overseas Trust (Schlumberger Research) and ICI for funding to TK, and to the EPSRC for a grant to BFGJ.

- [1] R. Raja, G. Sankar, S. Hermans, D. S. Shephard, S. Bromley, J. M. Thomas, B. F. G. Johnson, T. Maschmeyer, *Chem. Commun.* **1999**, 1571–1572.
- [2] R. Raja, T. Khimyak, J. M. Thomas, S. Hermans, B. F. G. Johnson, *Angew. Chem. Int. Ed.* **2001**, *40*, 4638–4642.
- [3] T. Nakajima, A. Ishiguro, Y. Wakatsuki, *Angew. Chem. Int. Ed.* **2000**, *39*, 1131–1134.
- [4] S. Hermans, T. Khimyak, B. F. G. Johnson, *J. Chem. Soc., Dalton Trans.* **2001**, 3295–3302.
- [5] R. D. Adams, W. Wu, *J. Cluster Sci.* **1991**, *2*, 271–290.
- [6] R. D. Adams, W. Wu, *J. Cluster Sci.* **1993**, *4*, 245–258.
- [7] D. Braga, F. Grepioni, P. J. Dyson, B. F. G. Johnson, P. Frediani, M. Bianchi, F. Piacenti, *J. Chem. Soc., Dalton Trans.* **1992**, 2565–2571.
- [8] B. F. G. Johnson, J. Lewis, S. W. Sankey, K. Wong, M. McPartlin, W. J. H. Nelson, *J. Organomet. Chem.* **1980**, *191*, C3–C7.
- [9] B. F. G. Johnson, J. Lewis, J. N. Nicholls, J. Puga, P. R. Raithby, M. J. Rosales, M. McPartlin, W. Clegg, *J. Chem. Soc., Dalton Trans.* **1983**, 277–290.
- [10] R. D. Adams, W. G. Wu, *Organometallics* **1993**, *12*, 1238–1242.
- [11] B. F. G. Johnson, T. Khimyak, *manuscript in preparation*.
- [12] L. J. Farrugia, *Organometallics* **1990**, *9*, 105–110.
- [13] B. N. Storhoff, H. C. Lewis, *Coord. Chem. Rev.* **1977**, *23*, 1–29.
- [14] C. Couture, D. H. Farrar, *J. Chem. Soc., Dalton Trans.* **1987**, 2245–2252.
- [15] F. A. Cotton, G. Wilkinson, *Advanced Inorganic Chemistry*, Wiley, New York, 5th ed., **1988**, ch. 19, p. 918.
- [16] S. Hermans, B. F. G. Johnson, *Chem. Commun.* **2000**, 1955–1956.
- [17] B. F. G. Johnson, J. Lewis, W. J. H. Nelson, J. N. Nicholls, J. Puga, P. R. Raithby, M. J. Rosales, M. Schröder, M. D. Vargas, *J. Chem. Soc., Dalton Trans.* **1983**, 2447–2457.
- [18] teXsan, Version 1.7. Molecular Structure Corporation, **1995**.
- [19] G. Sheldrick, *SHELX-97*, University of Göttingen, **1997**.
- [20] G. Sheldrick, *SHELXL-93*, University of Göttingen, **1993**.

Received August 19, 2002  
[I02467]